Science Translational Medicine
AAAS

A Central Role for Free Heme in the Pathogenesis of Severe Sepsis

Rasmus Larsen, *et al.*

Sci Transl Med **2**, 51ra71 (2010);
DOI: 10.1126/scitranslmed.3001118

Science Translational Medicine (print ISSN 1946-6234; online ISSN 1946-6242) is published weekly, except the last week in December, by the American Association for the Advancement of Science, 1200 New York Avenue NW, Washington, DC 20005.

SEPSIS

A Central Role for Free Heme in the Pathogenesis of Severe Sepsis

Rasmus Larsen,[1] Raffaella Gozzelino,[1] Viktória Jeney,[1] László Tokaji,[1] Fernando A. Bozza,[2,3] André M. Japiassú,[2,3] Dolores Bonaparte,[1] Moisés Marinho Cavalcante,[1]* Ângelo Chora,[1] Ana Ferreira,[1] Ivo Marguti,[1] Sílvia Cardoso,[1] Nuno Sepúlveda,[1,4] Ann Smith,[5] Miguel P. Soares[1†]

(Published 29 September 2010; Volume 2 Issue 51 51ra71)

Low-grade polymicrobial infection induced by cecal ligation and puncture is lethal in heme oxygenase-1–deficient mice (*Hmox1*$^{-/-}$), but not in wild-type (*Hmox1*$^{+/+}$) mice. Here we demonstrate that the protective effect of this heme-catabolizing enzyme relies on its ability to prevent tissue damage caused by the circulating free heme released from hemoglobin during infection. Heme administration after low-grade infection in mice promoted tissue damage and severe sepsis. Free heme contributed to the pathogenesis of severe sepsis irrespective of pathogen load, revealing that it compromised host tolerance to infection. Development of lethal forms of severe sepsis after high-grade infection was associated with reduced serum concentrations of the heme sequestering protein hemopexin (HPX), whereas HPX administration after high-grade infection prevented tissue damage and lethality. Finally, the lethal outcome of septic shock in patients was also associated with reduced HPX serum concentrations. We propose that targeting free heme by HPX might be used therapeutically to treat severe sepsis.

INTRODUCTION

Severe sepsis is a disease with limited treatment options that kills more than half a million individuals per year in the United States alone (*1*). Severe sepsis can develop from an unfettered immune response to microbial infection that leads to a systemic refractory drop in blood pressure, disseminated intravascular coagulation, multiple end-stage organ failure, and eventually, death (*2*). The physiological and molecular mechanisms that underlie the pathogenesis of severe sepsis remain poorly understood (*2*).

In most cases of microbial infection, the innate and adaptive immune systems allow for pathogen clearance and a return to homeostasis (*3*). In some cases, however, this host defense strategy, referred to as resistance to infection (*4*–*6*), can lead to irreversible tissue damage and compromise host viability (*7*). An alternative host defense strategy, referred to as tolerance to infection (*5*, *6*), can limit disease severity irrespective of pathogen load (*4*–*6*). Host genes conferring tolerance to infection include the stress-responsive enzyme heme oxygenase-1 (*Hmox1*), as previously demonstrated for malaria, the disease caused by *Plasmodium* infection (*8*).

Heme oxygenase-1 (HO-1) acts as the rate-limiting enzyme in the breakdown of heme (Fe protoporphyrin IX; FePPIX) into equimolar amounts of biliverdin, iron (Fe), and carbon monoxide (*9*). Induction of HO-1 expression in response to stress caused by microbial infection suppresses the development of severe sepsis in mice (*10*). This safeguarding action can act irrespective of pathogen load, relying instead on the cytoprotective effect of HO-1 against the excess free heme produced via hemolysis during infection.

Free heme induces programmed cell death in response to proinflammatory agonists, as demonstrated for tumor necrosis factor (TNF) (*8*, *11*). We refer to this phenomenon as "heme sensitization" to programmed cell death, because the cytotoxic effect of free heme is revealed only in the presence of other cytotoxic agonists (*8*, *11*). The molecular mechanism underlying the cytotoxic effect of free heme relies on its pro-oxidant activity (*8*, *11*), driven by the divalent Fe atom contained within its protoporphyrin IX ring, which can promote the production of free radicals via Fenton chemistry (*12*).

Given that free heme can cause tissue damage and hence compromise host tolerance to infection, we investigated whether limiting this deleterious effect can be used for therapeutic purposes to enhance host tolerance against microbial infections and prevent the development of severe sepsis.

RESULTS

HO-1 affords host tolerance against polymicrobial infection

Severe sepsis was produced in BALB/c mice by low-grade polymicrobial infection induced by cecal ligation and puncture (CLP). Using quantitative reverse transcription polymerase chain reaction (RT-PCR), we measured the expression of the *Hmox1* gene and found that it was induced in peritoneal infiltrating leukocytes, liver, lung, and kidney at various time points after CLP (Fig. 1A). Mortality increased from 13% in wild-type (*Hmox1*$^{+/+}$) mice to 80% in *Hmox1*-deficient (*Hmox1*$^{-/-}$) mice when both were subjected to low-grade CLP (Fig. 1B). Similar results were obtained in BALB/c severe combined immunodeficient (SCID) mice lacking B and T lymphocytes (Fig. 1B), demonstrating that the protective effect of HO-1 is not dependent on adaptive immunity. The mortality of heterozygous *Hmox1*$^{+/-}$ mice was similar

[1]Instituto Gulbenkian de Ciência, Rua da Quinta Grande 6, 2780-156 Oeiras, Portugal. [2]Intensive Care Unit, Instituto de Pesquisa Clínica Evandro Chagas, Fundação Oswaldo Cruz, 21040-900 Rio de Janeiro, Brazil. [3]D'Or Institute for Research and Education, 22281-100 Rio de Janeiro, Brazil. [4]Center of Statistics and Applications of the University of Lisbon, Campo Grande, 1749-016 Lisbon, Portugal. [5]Division of Molecular Biology and Biochemistry, University of Missouri, 5007 Rockhill Road, Kansas City, MO 64110, USA.
*Present address: Universidade Federal do Rio de Janeiro Campus Macaé–Instituto Macaé de Metrologia e Tecnologia, Macaé, Rio de Janeiro 27930-560, Brazil.
†To whom correspondence should be addressed. E-mail: mpsoares@igc.gulbenkian.pt

to that of *Hmox1*$^{+/+}$ mice (Fig. 1B). The higher mortality of *Hmox1*$^{-/-}$ versus *Hmox1*$^{+/+}$ mice was not attributable to the surgical procedure per se, as *Hmox1*$^{-/-}$ mice did not succumb to sham laparotomy, which mimicked CLP without polymicrobial infection.

The mortality of *Hmox1*$^{-/-}$ mice after CLP was associated with the development of multiple end-stage organ failure, a hallmark of severe sepsis (*2*). Plasma concentrations of aspartate aminotransferase (AST), blood urea nitrogen (BUN), and creatinine phosphokinase (CPK), markers of liver, kidney, and muscle dysfunction, respectively, were significantly increased in infected *Hmox1*$^{-/-}$ versus *Hmox1*$^{+/+}$ mice (Fig. 1C). Liver, kidney, and cardiac damage were confirmed by histological detection of centrolobular necrosis, tubular epithelial necrosis, and myocardial necrosis, respectively (Fig. 1D). This demonstrates that induction of HO-1 expression in response to polymicrobial infection limits tissue damage and the development of severe sepsis.

Exacerbated mortality of *Hmox1*$^{-/-}$ versus *Hmox1*$^{+/+}$ mice did not result from higher pathogen (bacterial) load, as assessed by comparing the number of colony-forming units (CFUs) in the peritoneum and blood (Fig. 1E), as well as in the liver, spleen, kidneys, and lungs (fig. S1). *Hmox1*$^{-/-}$ mice also succumbed when challenged with heat-killed bacteria (60% mortality), whereas *Hmox1*$^{+/-}$ and *Hmox1*$^{+/+}$ mice did not (0% mortality) (Fig. 1F). This demonstrates that HO-1 affords tolerance against polymicrobial infection (*5*, *6*) independently of its previously reported antimicrobial activity (*10*).

Production of several cytokines involved in the pathogenesis of severe sepsis [for example, TNF, interleukin-6 (IL-6), and IL-10] was similar in *Hmox1*$^{-/-}$ versus *Hmox1*$^{+/-}$ or *Hmox1*$^{+/+}$ mice subjected to low-grade CLP (fig. S2, A, D, and G). Likewise, peritoneal or bone marrow–derived monocytes/macrophages (Mø) from *Hmox1*$^{-/-}$ versus *Hmox1*$^{+/+}$ mice produced similar amounts of IL-6 when exposed in vitro to bacterial lipopolysaccharide (LPS) or to live bacteria (fig. S2, E and F), while producing slightly but significantly higher amounts of TNF when exposed to LPS (fig. S2B) but not to live bacteria (fig. S2C). Higher production of IL-10 also occurred in *Hmox1*$^{-/-}$ versus *Hmox1*$^{+/+}$ Mø exposed to LPS or to live bacteria (fig. S2, H and I). Because HO-1 regulates the expression of a subset of cytokines, including IL-10 (fig. S2, H and I) in response to bacterial agonists such as LPS (fig. S2H) or live bacteria (fig. S2I), we cannot exclude that this effect might contribute to the protective mechanism by which HO-1 suppresses the pathogenesis of severe sepsis.

When exposed to LPS and interferon-γ (IFN-γ), peritoneal Mø from naïve *Hmox1*$^{-/-}$ mice produced slightly but significantly higher amounts of nitric oxide (NO) than did *Hmox1*$^{+/+}$ peritoneal Mø (fig. S3A). Whether reduced NO production contributes to the protective action of HO-1 remains to be established.

HO-1 prevents free heme from eliciting severe sepsis

Free heme, the substrate of HO-1 activity, is cytotoxic to red blood cells and causes hemolysis (*13*). This produces cell-free hemoglobin and eventually more free heme (*14*) (that is, heme not contained within the heme pockets of hemoglobin). This definition of free heme does not preclude the association of heme with other proteins or lipids in a manner that does not control its ability to induce oxidative stress (*11*). We asked whether increased mortality of *Hmox1*$^{-/-}$ mice subjected to polymicrobial infection was associated with increased hemolysis, as well as with the accumulation of cell-free hemoglobin and/or free heme in plasma (*11*). When subjected to low-grade CLP, *Hmox1*$^{-/-}$ mice, but not *Hmox1*$^{+/+}$ mice, accumulated extracellular hemoglobin (Fig. 2A) and free heme in plasma (Fig. 2B), whereas plasma concentrations of the hemoglobin-binding protein haptoglobin (*15*) (Fig. 2A) and the heme-binding protein hemopexin (HPX) (*16*) were decreased (Fig. 2B).

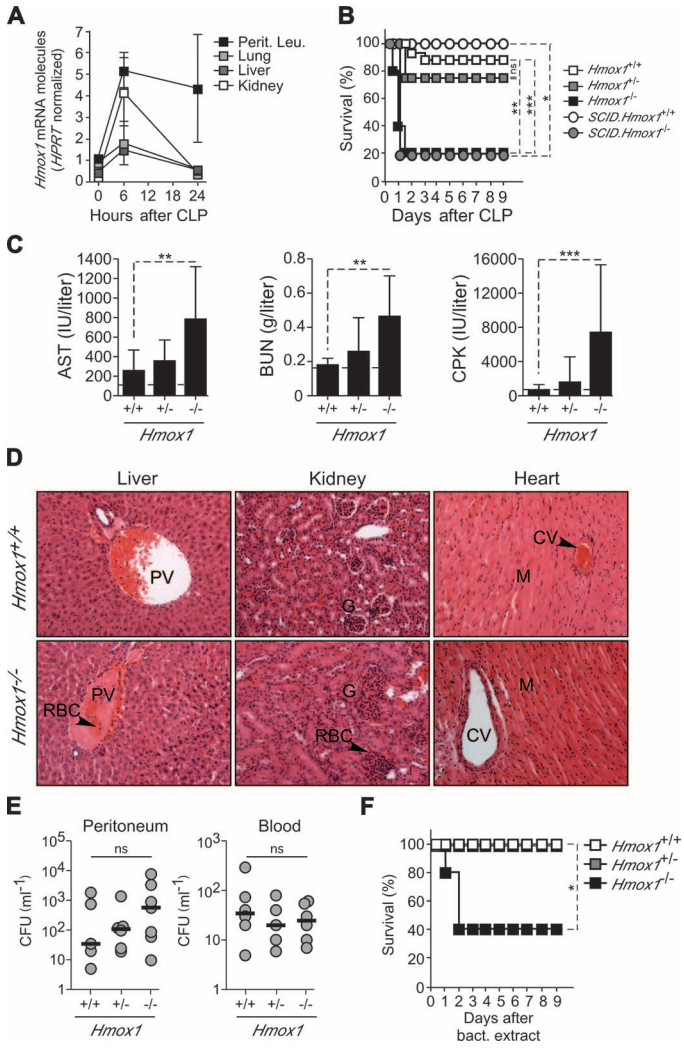

Fig. 1. HO-1 affords tolerance against polymicrobial infection in mice. (**A**) *Hmox1* messenger RNA (mRNA) expression in peritoneal leukocytes (Perit. leu.), lung, liver, and kidney after low-grade CLP in BALB/c mice, as determined by quantitative RT-PCR. Data are shown as mean ± SD (n = 3 per group). (**B**) Survival of *Hmox1*$^{+/+}$ (n = 15), *Hmox1*$^{+/-}$ (n = 12), *Hmox1*$^{-/-}$ (n = 10), *SCID.Hmox1*$^{+/+}$ (n = 5), and *SCID.Hmox1*$^{-/-}$ (n = 5) BALB/c mice after low-grade CLP. (**C**) Serological markers of organ injury in *Hmox1*$^{+/+}$ (n = 15 to 17), *Hmox1*$^{+/-}$ (n = 10 to 13), and *Hmox1*$^{-/-}$ (n = 6) BALB/c mice 24 hours after low-grade CLP. Data are shown as mean ± SD. Dashed lines indicate basal plasma concentrations in naïve wild-type BALB/c mice. IU, international units. (**D**) Representative examples of hematoxylin and eosin (H&E)–stained liver, kidney, and heart tissues from *Hmox1*$^{+/+}$ and *Hmox1*$^{-/-}$ mice after low-grade CLP. Magnification, ×400. Arrows indicate red blood cells (RBCs) associated with vascular congestion and/or thrombosis. CV, coronary vessel; M, myocardium; PV, portal vein; G, glomerulus. (**E**) Bacterial load (CFU) in the peritoneum and blood of mice subjected to low-grade CLP (12 hours after CLP). Circles represent individual mice. Bars represent median values. ns, not significant. (**F**) Survival of *Hmox1*$^{+/+}$ (n = 7), *Hmox1*$^{+/-}$ (n = 6), and *Hmox1*$^{-/-}$ (n = 5) BALB/c mice after intraperitoneal administration of heat-killed bacteria (Bact.). *P < 0.05; **P < 0.01; ***P < 0.001; ns, not significant.

We then asked whether accumulation of free heme in plasma contributes to the pathogenesis of severe sepsis. Heme administration to wild-type (*Hmox1*$^{+/+}$) mice subjected to low-grade CLP led to severe sepsis (77% mortality) (Fig. 2C), characterized by multiple end-stage organ failure, as revealed serologically by increased AST, BUN, and CPK plasma concentrations (Fig. 2D). Organ damage was confirmed histologically (Fig. 2E). Heme administration to naïve wild-type (*Hmox1*$^{+/+}$) mice, although not lethal per se (0% mortality), elicited kidney, but not liver or cardiac, damage (Fig. 2D). Heme administra-

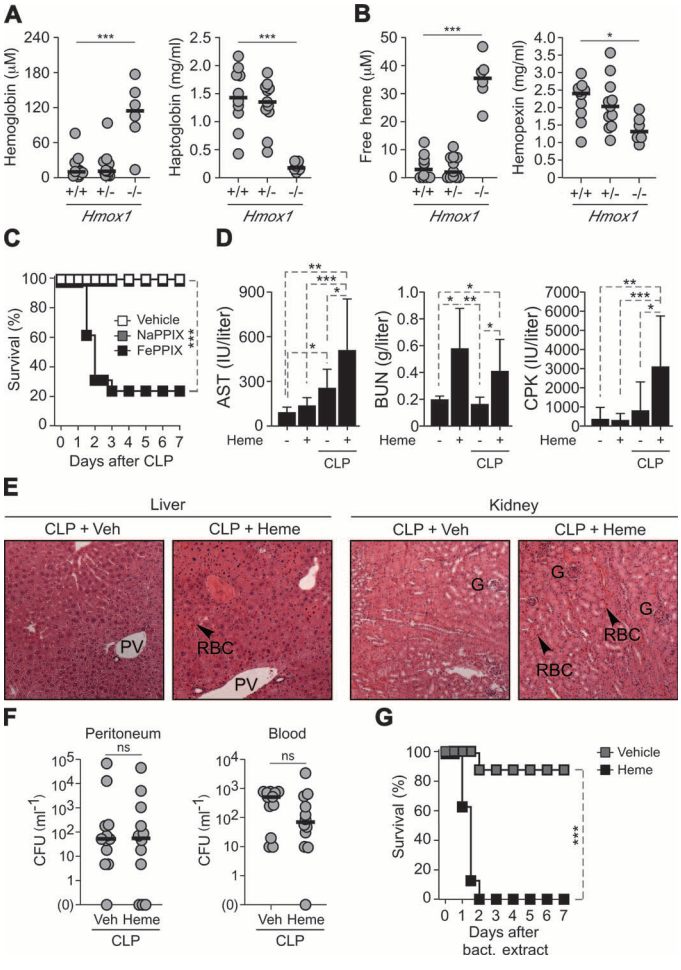

Fig. 2. HO-1 prevents heme-driven severe sepsis. (**A**) Hemoglobin and haptoglobin plasma concentrations in *Hmox1*$^{+/+}$ (n = 10), *Hmox1*$^{+/-}$ (n = 11), and *Hmox1*$^{-/-}$ (n = 6) BALB/c mice 12 hours after low-grade CLP. (**B**) Free heme and HPX plasma concentrations in *Hmox1*$^{+/+}$ (n = 10), *Hmox1*$^{+/-}$ (n = 11), and *Hmox1*$^{-/-}$ (n = 6) BALB/c mice, 12 hours after low-grade CLP. (**C**) Survival of *Hmox1*$^{+/+}$ BALB/c mice after low-grade CLP. When indicated, mice received vehicle (n = 6), protoporphyrin IX (NaPPIX; n = 8), or heme (FePPIX; n = 13). Protoporphyrins were administered (15 mg/kg ip) at 2, 12, and 24 hours after CLP. Dotted line shows statistical comparison of vehicle- and FePPIX-treated animals. (**D**) Measurement of serum AST, BUN, and CPK. Mice were treated as in (C), and serum biochemistry was analyzed 24 hours after low-grade CLP. Data are shown as mean ± SD (eight to nine mice per group). IU, international units. (**E**) Representative examples of H&E staining (magnification, ×400) of tissue samples taken 24 hours after low-grade CLP from mice that received heme described as in (C). Arrows indicate red blood cells (RBC). PV, portal vein; G, glomerulus. Samples are representative results of three mice in each group. (**F**) Bacterial load in the peritoneum and blood of mice (n = 12 per group) treated as described in (C), 12 to 24 hours after CLP. Veh, vehicle; Heme, FePPIX. (**G**) Survival of BALB/c wild-type (*Hmox1*$^{+/+}$) mice after intraperitoneal administration of a sublethal bolus of heat-killed bacteria (*E. coli*) followed by heme administration as in (C) (eight mice per group). Circles represent individual mice. Bars represent median values. *P < 0.05; **P < 0.01; ***P < 0.001; ns, not significant.

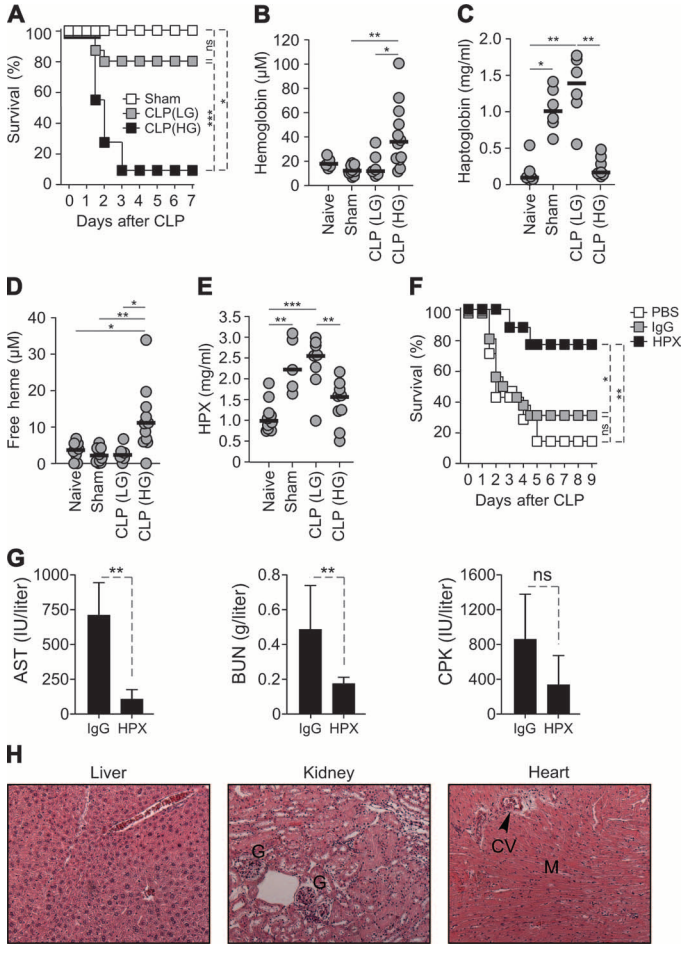

Fig. 3. Free heme promotes the pathogenesis of severe sepsis. (**A**) Survival of wild-type (*Hmox1*$^{+/+}$) BALB/c mice subjected to "sham" laparotomy (n = 3), low-grade (LG) (n = 15) CLP, or high-grade (HG) (n = 11) CLP. (**B** to **E**) Hemoglobin (B), haptoglobin (C), free heme (D), or HPX (E) plasma concentrations in naïve (n = 6 to 8) mice or 12 hours after sham laparotomy (n = 10), LG CLP (n = 6), or HG CLP (n = 11 to 12). Circles represent individual mice. Bars represent median values. (**F**) Survival of wild-type (*Hmox1*$^{+/+}$) BALB/c mice subjected to high-grade CLP. Mice received purified rabbit HPX (50 mg/kg ip; n = 9), purified rabbit polyclonal IgG (50 mg/kg ip; n = 16), or vehicle (intraperitoneally, PBS; n = 7) at 2, 12, 24, and 36 hours after CLP. (**G**) Serological markers of organ injury in mice treated as in (F). Measurements were made in serum from IgG-treated mice at the time of death (36 hours) and in HPX-treated mice at the end of the experiment (day 11). Results shown are the mean ± SD (n = 5 to 6 mice per group). (**H**) Representative H&E staining (magnification, ×400) in mice treated as in (F). Samples are representative of three mice. CV, coronary vessel; G, glomerulus. M, myocardium. Samples are representative results of three mice in each group. HPX-treated mice in (G) and (H) were analyzed 11 days after CLP. Control IgG-treated mice in (G) and (H) were analyzed 24 to 36 hours after CLP (time of death). *P < 0.05; **P < 0.01; ***P < 0.001; ns, not significant.

tion was also not lethal in mice subjected to sham laparotomy (0% mortality). Moreover, "iron-free" protoporphyrin IX failed to cause organ damage or to precipitate severe sepsis when administered to mice subjected to low-grade CLP (0% mortality) (Fig. 2C). These observations demonstrate that free heme can precipitate the onset of severe sepsis in mice subjected to an otherwise benign (nonlethal) polymicrobial infection. They also reveal that the kidney is particularly vulnerable to the damaging effects of free heme.

The number of CFUs in the peritoneum and blood was similar in mice subjected to low-grade CLP whether or not they received heme thereafter (Fig. 2F). This demonstrated that the ability of free heme to precipitate severe sepsis in mice (Fig. 2C) was not associated with increased pathogen load (Fig. 2F), thus revealing that free heme compromised host tolerance against polymicrobial infection. This notion was strongly supported by the observation that administration of free heme to wild-type (*Hmox1*$^{+/+}$) mice subjected to a sublethal dose of heat-killed bacteria led to 100% mortality, as compared to 12.5% mortality in control mice receiving vehicle (Fig. 2G).

We then asked whether the deleterious effect of free heme could be attributed to its previously described action on polymorphonuclear (PMN) cells (*17*). The numbers of peritoneal-infiltrating CD45^{+}CD11b^{+}GR1^{+} PMN cells in *Hmox1*$^{-/-}$ mice subjected to low-grade CLP were two to threefold higher than those in *Hmox1*$^{+/-}$ and *Hmox1*$^{+/+}$ mice (figs. S5 and S6, A and B). This was not the case for peritoneal natural killer (NK), T, or B cells (fig. S6, C to E). Expression of the phagocytic NADPH (reduced form of nicotinamide adenine dinucleotide phosphate) oxidase gp91^{phox} in peritoneal infiltrating leukocytes was also higher in *Hmox1*$^{-/-}$ versus *Hmox1*$^{+/+}$ mice (fig. S5B). This effect was attributed to the increased numbers of PMN cells in *Hmox1*$^{-/-}$ versus *Hmox1*$^{+/+}$ mice and was associated with enhanced oxidative activity in peritoneal leukocytes from *Hmox1*$^{-/-}$ mice relative to *Hmox1*$^{+/+}$ mice (fig. S5, C and D). Whereas heme administration to naïve *Hmox1*$^{+/+}$ mice can elicit peritoneal PMN cell infiltration (fig. S5E) (*17*), this effect was negligible when heme was administered to mice subjected to low-grade CLP (fig. S5E). Although these data suggest that heme-driven PMN cell activation does not play a major role in the pathogenesis of severe sepsis, we cannot exclude that other putative effects of free heme on PMN cells, such as degranulation, might act in a detrimental manner to promote the pathogenesis of severe sepsis.

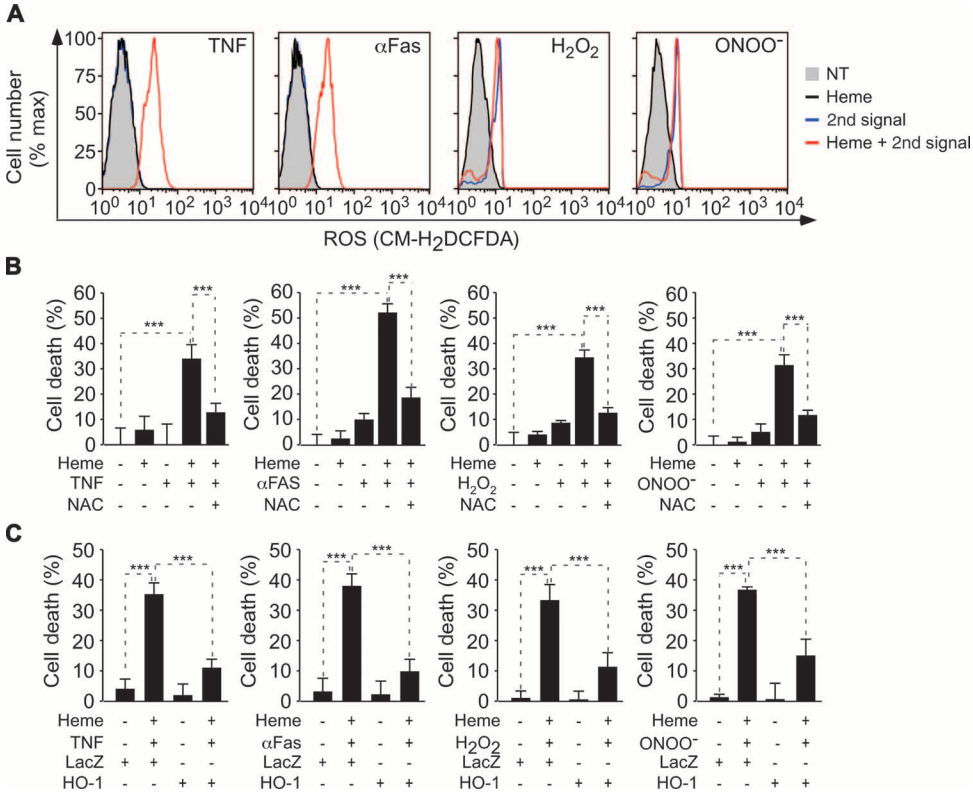

Fig. 4. The oxidative effect of free heme sensitizes hepatocytes to programmed cell death. (**A**) Primary BALB/c hepatocytes were either untreated (NT) or exposed to heme (5 μM, 1 hour) plus mouse recombinant TNF (5 ng/ml, for 16 hours), antibody against Fas (0.5 μg/ml, for 4 hours), H_2O_2 (125 μM, for 8 hours), or the $ONOO^-$ donor SIN-1 (100 μM, for 24 hours). Production of free radicals was determined by flow cytometry with CM-H_2DCFDA. 2nd signal refers to TNF, antibody against Fas, H_2O_2, or $ONOO^-$, as specified for each panel. (**B**) Percentage of cell death in primary hepatocytes treated as in (A). When indicated (+), hepatocytes were pretreated with the antioxidant NAC (10 mM, for 4 hours). Cell viability was determined by crystal violet staining. (**C**) Percentage of cell death in primary hepatocytes treated as in (A). When indicated (+), hepatocytes were transduced with a *LacZ*- or *Hmox1*-encoding Rec.Ad. Cell viability was determined as in (B). Data are representative of three independent experiments with hepatocytes isolated from different mice. Bars indicate mean ± SD of $n = 5$ to 6 independent samples per group. *$P < 0.05$; **$P < 0.01$; ***$P < 0.001$.

Free heme is a critical component in the pathogenesis of severe sepsis

When subjected to high-grade CLP (>90% mortality) (Fig. 3A), wild-type (*Hmox1*$^{+/+}$) mice displayed abnormal red blood cell morphology (poikilocytosis) (fig. S4). This was associated with the accumulation of cell-free hemoglobin in plasma (Fig. 3B), compared to mice subjected to low-grade CLP (<20% mortality) (Fig. 3, A and B, and fig. S4). Moreover, there was a decrease in haptoglobin plasma concentrations in *Hmox1*$^{+/+}$ mice subjected to high-grade CLP compared to mice subjected to low-grade CLP (Fig. 3C), confirming that hemolysis occurs in response to high-grade but not low-grade infection. Similarly, the concentration of free heme in plasma increased (Fig. 3D), whereas HPX plasma concentration decreased (Fig. 3E), in mice subjected to high-grade relative to low-grade CLP. Given that mortality in response to polymicrobial infection is associated with high concentrations of free heme and low concentrations of HPX in plasma, we hypothesized that one might be able to prevent the onset of severe sepsis by restoring HPX plasma concentration, so that HPX is available to neutralize the rising amounts of free heme. Administration of purified HPX to wild-type (*Hmox1*$^{+/+}$) mice subjected to high-grade CLP reduced the mortality level

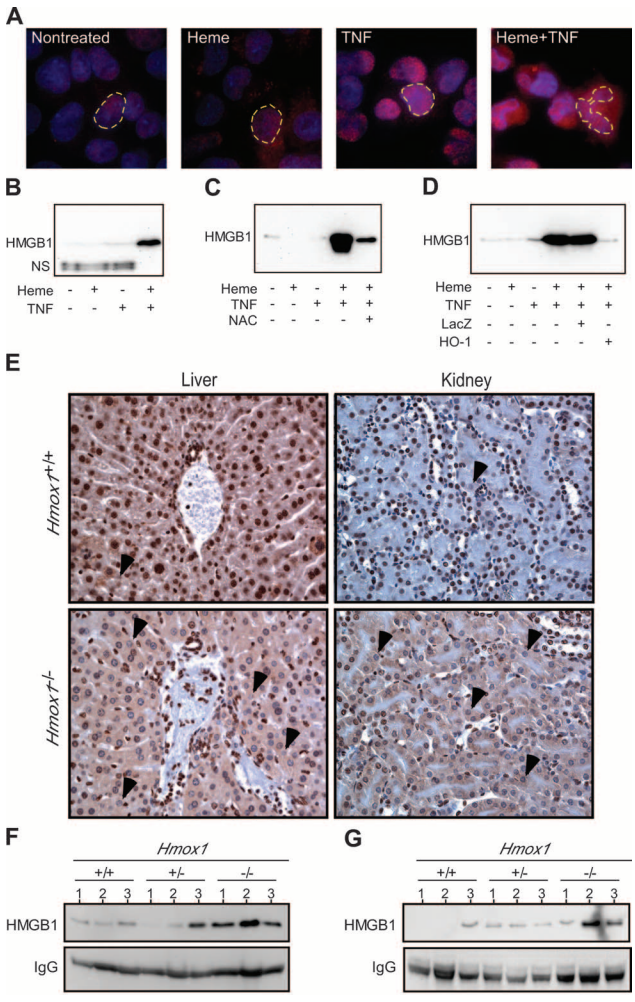

Fig. 5. Free heme triggers the release of HMGB1 from hepatocytes. (**A**) HMGB1 (red) and DNA (blue) in mouse Hepa1-6 hepatocytes exposed to vehicle (Nontreated), free heme (40 μM, for 1 hour), TNF (50 ng/ml, for 3 hours), or heme (40 μM, for 1 hour) plus TNF (50 ng/ml, for 3 hours). Magnification, ×400. Images are representative of three independent experiments. One nucleus per field is outlined (dotted line). (**B**) HMGB1 was measured by Western immunoblotting of proteins in the supernatants of primary mouse (BALB/c) hepatocytes that were exposed to heme (5 μM, for 1 hour) and TNF (5 ng/ml, for 16 hours) in culture. A representative result from two independent experiments is shown. NS, nonspecific band. (**C**) HMGB1 was measured by Western immunoblotting of proteins in the supernatants of mouse Hepa1-6 hepatocytes exposed to heme and TNF as described in (A). When indicated, cells were pretreated with the antioxidant NAC (10 mM; for 4 hours). A representative result from two independent experiments is shown. (**D**) HMGB1 was measured by Western immunoblotting of proteins in the supernatants of mouse Hepa1-6 hepatocytes treated with heme and TNF as in (A) and either transduced or not transduced with *LacZ* or *Hmox1* Rec.Ad. Blots are representative of two independent experiments. (**E**) HMGB1 staining in the liver and kidney from *Hmox1*$^{+/+}$ and *Hmox1*$^{-/-}$ mice 24 hours after CLP. One of three representative samples are shown. Samples were counterstained with hematoxylin. Magnification, ×400. Arrows indicate representative nuclei from which HMGB1 underwent full translocation from the nucleus to the cytoplasm and extracellular space. (**F** and **G**) HMGB1 and Ig heavy chain (IgG) were detected by Western blot in the peritoneal cavity (F) or plasma (G) of *Hmox1*$^{+/+}$, *Hmox1*$^{+/-}$, or *Hmox1*$^{-/-}$ mice 12 hours after low-grade CLP. Numbers indicate individual animals (n = 3 per genotype).

to 22%, compared to 86 and 69% in control mice that received phosphate-buffered saline (PBS) (the HPX vehicle) or immunoglobulin G (IgG), respectively (Fig. 3F). The protective effect of HPX was associated with the return of liver, kidney, and cardiac function to homeostatic levels, as assessed by AST, BUN, and CPK plasma concentrations, respectively (Fig. 3G), and as confirmed histologically (Fig. 3H). In contrast, control mice that received a non–heme-binding protein (IgG) after high-grade CLP succumbed to liver, cardiac, and kidney failure, as assessed by AST, BUN, and CPK plasma concentrations, respectively (Fig. 3G).

Free heme elicits programmed cell death

We have previously shown that free heme can promote programmed cell death in response to TNF (*8*). We asked whether this effect is extended to other agonists involved in the pathogenesis of severe sepsis. Because hepatic failure is a central component of severe sepsis, we tested whether free heme induces oxidative stress and TNF-mediated programmed cell death in primary mouse hepatocytes in vitro. When exposed to free heme, hepatocytes did not produce significant amounts of intracellular free radicals, as assessed by flow cytometry with a broad free radical probe (Fig. 4A). However, when exposed to free heme and TNF (Fig. 4A) (*8*) or free heme plus Fas cross-linking (which activates the Fas signaling transduction pathway), hepatocytes produced large amounts of intracellular free radicals (Fig. 4A). This effect was not observed when hepatocytes were exposed to free heme and oxidizing agents such as hydrogen peroxide (H_2O_2) or peroxynitrite ($ONOO^-$), which are sufficient to cause free radical accumulation in hepatocytes (Fig. 4A). Primary hepatocytes did not undergo programmed cell death when exposed to TNF, Fas cross-linking, H_2O_2, or $ONOO^-$ (Fig. 4B) (*8*), whereas programmed cell death was readily induced in cells treated with free heme first and then TNF, Fas cross-linking, H_2O_2, or $ONOO^-$ (Fig. 4B). These observations suggest that the redox activity of the heme Fe atom underlies its cytotoxicity, presumably by catalyzing the production of free radicals through Fenton chemistry (*12*). Consistent with this hypothesis, the antioxidant *N*-acetyl-cysteine (NAC) protected hepatocytes from programmed cell death in the presence of free heme and TNF, Fas ligand, H_2O_2, or $ONOO^-$ (Fig. 4B). These observations reveal that the pathological effects of free heme, namely, its ability to synergize with other cytotoxic agonists to cause tissue damage, can be extended to a variety of agonists other than TNF (*11*), including some previously implicated in the pathogenesis of severe sepsis.

Transduction of hepatocytes with a recombinant adenovirus (Rec.Ad.) that expresses HO-1 (fig. S7) was protective against programmed cell death in the presence of free heme and TNF, Fas cross-linking, H_2O_2, or $ONOO^-$, when compared with control hepatocytes transduced with a Rec.Ad. that expresses *LacZ* (Fig. 4C). We have previously shown that the cytoprotective effect of HO-1 is associated with inhibition of free radical production (*8*), suggesting that HO-1 acts as an antioxidant to suppress the cytotoxic effects of free heme (*8*).

Heme triggers HMGB1 release in vitro and in vivo

We reasoned that the cytotoxic effect of free heme might precipitate severe sepsis by eliciting tissue damage per se, as well as by promoting the release of high mobility group box 1 (HMGB1), an endogenous proinflammatory ligand (*18*) involved in the pathogenesis of severe sepsis (*19*) and previously linked to HO-1 (*20*). In untreated primary hepatocytes, HMGB1 expression was mainly restricted to the nucleus (Fig. 5A). However, when hepatocytes were exposed in vitro to free heme plus TNF, HMGB1 was translocated from the nucleus to the

cytoplasm (Fig. 5A) and released extracellularly (Fig. 5B). This was not the case when hepatocytes were exposed to either free heme or TNF alone (Fig. 5, A and B). Extracellular HMGB1 release was suppressed by the antioxidant NAC (Fig. 5C), as well as by HO-1 overexpression (Fig. 5D). These observations reveal that the oxidative effect of free heme promotes HMGB1 release from hepatocytes, an effect suppressed by HO-1.

Next, we asked whether HO-1 would prevent HMGB1 release from damaged tissue in vivo (*18*), as suggested in previous studies (*20*). In *Hmox1*$^{-/-}$ mice subjected to low-grade CLP there was translocation of HMGB1 into the cytoplasm, as assessed in the liver and kidney (Fig. 5E), whereas translocation was less pronounced in wild-type (*Hmox1*$^{+/+}$) mice (Fig. 5E). This effect was associated with the systemic release of HMGB1 into the peritoneum and plasma of *Hmox1*$^{-/-}$ relative to *Hmox1*$^{+/+}$ mice (Fig. 5, F and G). The relative amount of peritoneal or plasma IgG was unchanged in *Hmox1*$^{-/-}$ versus *Hmox1*$^{+/+}$ mice (Fig. 5, F and G).

HPX neutralizes the cytotoxic effect of free heme

We next sought to determine whether HPX, which binds tightly to heme (K_d <1 pM) in a manner that dampens its pro-oxidant activity (*21*), can also prevent heme-induced tissue damage (Fig. 3, F to H) (*16*). The ability of free heme to sensitize hepatocytes in vitro such that they produced high amounts of free radicals in response to TNF was inhibited when heme was bound to HPX (Fig. 6A). Moreover, the ability of free heme to sensitize hepatocytes to undergo programmed cell death in response to TNF was also inhibited once heme was bound to HPX (Fig. 6B). Similar results were obtained with primary human hepatocytes in that HPX prevented heme sensitization to programmed cell death in response to TNF (Fig. 6C). Accordingly, HPX-bound heme also failed to promote HMGB1 release from primary mouse hepatocytes in vitro (Fig. 6D). Similarly, HPX-bound heme also failed to promote HMGB1 release from primary human hepatocytes in response to TNF (Fig. 6E). The increased molecular weight of the cell-free HMGB1 released from primary human hepatocytes is most likely attributed to posttranscriptional HMGB1 modifications, such as phosphorylation. Together, these observations suggest that HPX suppresses the cytotoxic effects of free heme in both mouse and human hepatocytes.

Low HPX serum concentration is associated with organ dysfunction and fatal outcome in septic shock patients

Given that HPX plasma concentration is reduced in mice that succumb to severe sepsis (Fig. 3E), we asked whether this would also be the case in patients that succumb to septic shock (*22*). In a cohort of 52 patients (table S1), HPX serum concentration within 48 hours of presentation with septic shock was positively associated with patient survival time (Fig. 6F). That is, patients with lower HPX serum concentrations succumbed at earlier time points compared to patients with higher HPX serum concentrations (Fig. 6F). This observation allowed us to extrapolate the probability of survival/mortality as a function of HPX serum concentration (Fig. 6G), in keeping with the observation that HPX serum concentration within 48 hours of septic shock diagnosis was higher in patients that survived septic shock compared to nonsurvivors (Fig. 6H). Finally, there was an inverse correlation between HPX serum concentration and severity of organ dysfunction,

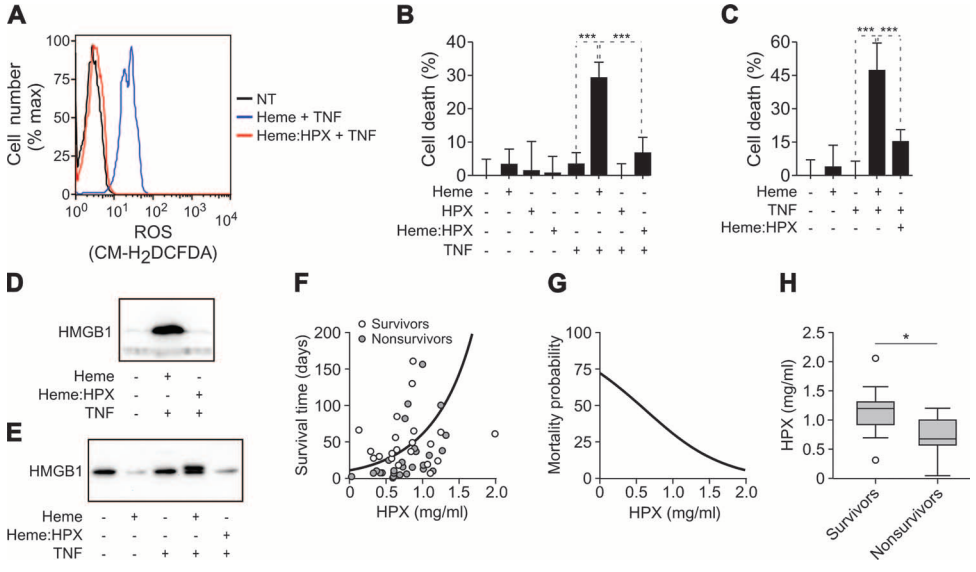

Fig. 6. HPX suppresses the cytotoxic effect of free heme. (**A**) Primary BALB/c hepatocytes were untreated (NT) or exposed to heme (5 μM) or HPX-heme complexes (5 μM, for 1 hour) and TNF (5 ng/ml, for 16 hours). Production of free radicals was determined by flow cytometry with the broad free radical probe CM-H_2DCFDA. (**B**) Primary BALB/c hepatocytes were treated as in (A), exposed to heme (5 μM), HPX (5 μM), or heme-HPX complexes (5 μM, for 1 hour) and, when indicated, to TNF (5 ng/ml; for 16 hours). Cell viability was determined by crystal violet staining. Results shown are the mean ± SD from six samples in one of two independent experiments with hepatocytes pooled from three mice. (**C**) Primary human hepatocytes were exposed to heme (10 μM; 1 hour) or heme-HPX complexes (10 μM, 1 hour), and then to TNF (10 ng/ml, 8 hours). Cell viability was determined by crystal violet staining. Results shown are the mean ± SD from six samples in one experiment representative of four independent experiments. (**D**) HMGB1 was measured by Western blotting of proteins in the supernatants of primary mouse (BALB/c) hepatocytes treated as in (A). Blots are representative of two independent experiments. (**E**) HMGB1 measured by Western blotting in the supernatants of primary human hepatocytes treated as in (C). (**F**) Survival time (see Materials and Methods) of patients developing septic shock versus prediction of best-fitted model. The solid line refers to the expected median survival time as a function of HPX serum concentration at the time of septic shock diagnosis, predicted by the best model for survival time (based on lognormal distribution). Gray circles represent individuals that succumbed during hospitalization (nonsurvivors). White circles represent individuals that survived septic shock and left the hospital at the times indicated. $P < 0.05$ for the respective effect. (**G**) Expected mortality probability at day 28, plotted as a function of HPX serum concentration at the time of septic shock diagnosis, predicted by the best model for survival time (based on lognormal distribution). (**H**) Box plot representation of HPX serum concentration at the time of septic shock diagnosis in a cohort of 52 patients, including survivors ($n = 34$) and nonsurvivors ($n = 18$). Data represent mean [interquartile range (IQR), 25 to 75%]. *$P < 0.05$.

as defined by the sequential organ failure assessment (SOFA) score (*23*) (table S2). Overall, these observations support the notion that HPX serum concentration defines the extent of tissue damage (organ dysfunction) and hence the outcome of septic shock in humans.

DISCUSSION

An infected host has two distinct evolutionarily conserved defense strategies that limit disease severity. The best-characterized of these two strategies relies on the capacity of the host immune system to contain and reduce its pathogen load. This defense strategy is referred to as host resistance to infection (*6*). The other defense strategy acts irrespective of pathogen load and relies instead on limiting tissue damage caused directly or indirectly by the pathogen and/or by the immune response elicited by that pathogen. This defense strategy, referred to as host tolerance to infection (*6*), has long been recognized in plants (*5*), but only more recently in flies (*6*) and mice (*24*).

Blood-borne pathogens can cause hemolysis (*25*) and hence lead to accumulation of extracellular hemoglobin in the circulation. Oxidation of cell-free hemoglobin can be highly deleterious to the host in at least three ways. First, it can exacerbate inflammation (*26*). Second, it can release heme (Figs. 2, A and B, and 3D) (*14*), a putative source of iron that can promote microbial growth (*27*). Third, as shown herein, free heme can be highly cytotoxic in the presence of proinflammatory agonists (Fig. 4B) (*11*), causing irreversible tissue damage and organ failure (Fig. 2, D and E), the hallmarks of severe sepsis (*2*) (Fig. 7).

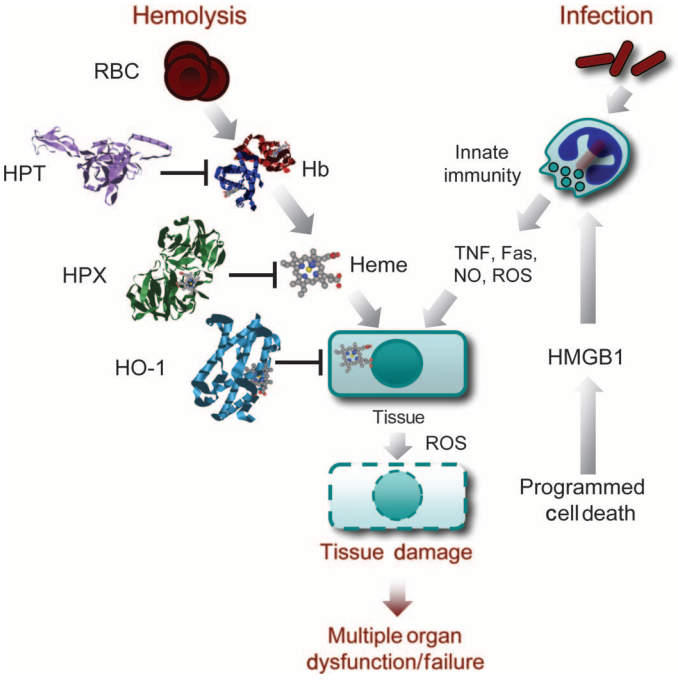

Fig. 7. Role of free heme in the pathogenesis of severe sepsis. The pathogenesis of severe sepsis is associated with hemolysis, which involves the release of hemoglobin (Hb) from red blood cells (RBC). Oxidation of cell-free Hb leads to the release of its prosthetic heme groups. This pathological event can be prevented by the acute-phase protein haptoglobin (HPT), whereas free heme can be captured by the acute-phase protein HPX. Once the concentration of HPT and/or HPX in serum decreases below a certain threshold level, free heme accumulates in plasma and can sensitize cells in parenchymal tissues to undergo programmed cell death in response to a variety of proinflammatory agonists. This leads to the release of endogenous proinflammatory ligands from damaged tissues, for example, HMGB1. Expression of the stress-responsive enzyme HO-1 in parenchymal cells affords cytoprotection against free heme, thus suppressing tissue damage and ultimately multiple-organ dysfunction/failure.

That heme-driven tissue damage can contribute to the pathogenesis of severe sepsis is suggested by four independent lines of evidence. First, exacerbated mortality of *Hmox1*$^{-/-}$ mice subjected to microbial infection (Fig. 1B) correlated with the accumulation of free heme in the plasma (Fig. 2B). Second, administration of free heme to wild-type (*Hmox1*$^{+/+}$) mice subjected to low-grade (nonlethal) microbial infection was sufficient to elicit a lethal form of severe sepsis (Fig. 2C). Third, free heme accumulated in the plasma of wild-type (*Hmox1*$^{+/+}$) mice subjected to high-grade (lethal), but not low-grade, microbial infection (Fig. 3, A and D). Fourth, sequestration of free heme by HPX suppressed the development of severe sepsis in wild-type (*Hmox1*$^{+/+}$) mice subjected to high-grade microbial infection (Fig. 3, F to H).

There are a number of cytoprotective mechanisms against the deleterious effects of free heme (*8*, *11*, *16*, *28*). These include the plasma protein HPX, which binds free heme and neutralizes its oxidative (Fig. 6A) and hence cytotoxic (Fig. 6, B and C) effects (*16*) (Fig. 7). As shown, the lethal outcome of severe sepsis in mice (Fig. 3E) and septic shock in humans is associated with decreased concentration of circulating HPX (Fig. 6F). Therefore, we reasoned that administration of exogenous HPX might be used therapeutically to increase tolerance to infection and hence prevent the development of severe sepsis in mice, which we found to be the case (Fig. 3, F to H). It is likely that a similar approach will translate into the treatment of severe sepsis in humans, given the observation that low concentrations of circulating HPX are associated with septic shock lethality in humans as well (Fig. 6, F to H). One cannot exclude at this point that in addition to preventing the cytotoxic effects of free heme, HPX (*29*) might exert anti-inflammatory effects that contribute to its protective effect.

The salutary effect of HPX most probably requires the expression of HO-1 to catabolize HPX-bound heme (Fig. 7). This would explain why, despite the presence of HPX, HO-1–deficient (*Hmox1*$^{-/-}$) mice are highly susceptible to immune-mediated inflammatory diseases (*30*), including endotoxic shock (*31*) and polymicrobial infection (*10*) (Fig. 1B), in which lack of adequate HPX-bound heme catabolism leads to irreversible tissue damage, end-stage organ dysfunction, and eventually to death (*32*, *33*).

The protective effect of HO-1 against polymicrobial infection has previously been attributed to the antimicrobial activity of carbon monoxide (*10*), one of the end products of heme catabolism carried out by HO-1 (*9*). This would suggest that HO-1 affords some level of resistance against polymicrobial infection. Two independent lines of evidence support the notion that HO-1 also affords tolerance against polymicrobial infection: First, mice that can induce the expression of HO-1 (*Hmox1*$^{+/+}$) in response to polymicrobial infection (Fig. 1A) survive (Fig. 1B) when subjected to the same pathogen load (Fig. 1E) that kills *Hmox1*$^{-/-}$ mice (Fig. 1B). Second, *Hmox1*$^{-/-}$ but not *Hmox1*$^{+/+}$ mice succumb to death even when challenged with heat-killed bacteria (Fig. 1F) (*31*, *33*). These observations provide mechanistic evidence for the proposed protective effect of HO-1 expression in the outcome of severe sepsis and septic shock (*34*).

The mechanism by which HO-1 affords tolerance against microbial infections relies to a large extent on its ability to suppress the del-

eterious effect of free heme (Fig. 4, A and B) produced during the course of infection (Figs. 3D and 7). This notion is strongly supported by the observation that HO-1 protected mouse cells from the cytotoxic effects of free heme (Fig. 4C), and should prevent irreversible tissue damage, multiple organ dysfunction, and host death (Fig. 1, C and D). Because this protective effect of HO-1 does not interfere with pathogen load (Fig. 1E), we conclude that HO-1 promotes, whereas extracellular heme compromises, host tolerance to polymicrobial infection.

The findings from the studies reported here potentially can be translated into several clinical applications for monitoring and treatment of sepsis. In the clinical setting, monitoring the patients' levels of circulating heme and/or HPX might be used to predict the likelihood of a fatal outcome in each case of severe sepsis (Fig. 6G). In addition, the development of strategies that mitigate the deleterious effects of free heme might also be used therapeutically to prevent the all-too-common lethal outcome of severe sepsis.

MATERIALS AND METHODS

Mice and genotyping

BALB/c, BALB/c.SCID, BALB/c.*Hmox1*$^{+/-}$, and BALB/c.SCID.*Hmox1*$^{+/-}$ mice were maintained under specific pathogen-free conditions according to the Animal Care Committee of the Instituto Gulbenkian de Ciência. All animal protocols were approved by the "Direcção Geral de Veterinaria" of the Portuguese government. BALB/c.*Hmox1*$^{+/-}$ mice were generated originally by S. F. Yet (Pulmonary and Critical Care Division, Brigham and Women's Hospital, Boston, MA) by disruption of exon 3 in the *Hmox1* locus (*35*). Mice were backcrossed 10 times into the BALB/c background. Heterozygous (*Hmox1*$^{+/-}$) breeding pairs yield ~8% viable and otherwise healthy homozygous HO-1–deficient mice (*35*). Littermate *Hmox1*$^{-/+}$ and *Hmox1*$^{+/+}$ mice were used as controls. Mice were genotyped by PCR. Briefly, a 400–base-pair (bp) PCR product spanning the 5′ flanking region of the neomycin complementary DNA (cDNA) in the *Hmox1* locus was amplified from genomic DNA with the following primers: 5′-TCTTGACGAGTTCTTCTGAG-3′ and 5′-ACGAAGTGACGCCATCTGT-3′ (*35*). For the endogenous *Hmox1* locus, 5′-GGTGACAGAAGAGGCTAAG-3′ and 5′-CTGTAACTCCACCTCCAAC-3′ primers were used to amplify a 456-bp product. PCRs were repeated at least two times before experiments were performed and were carried out after experiments to confirm genotypes.

Cell culture

Primary mouse peritoneal leukocytes were obtained by peritoneal lavage with ice-cold apyrogen PBS (Sigma). Briefly, leukocytes were washed in PBS and resuspended in RPMI 1640 Glutamax I (Gibco) supplemented with 5% fetal bovine serum, penicillin (50 U/ml), and streptomycin (50 μg/ml) (Life Technologies). For cytokine measurements, cells (2.5×10^4) were plated in flat-bottom 96-well microtiter plates (Techno Plastic Products AG) (100 μl, 2 hours, 37°C); nonadherent cells were removed, and adherent cells, that is, Mø, were activated with bacterial LPS (Sigma, *Escherichia coli* serotype 0127:B8) for 6 or 24 hours. Bone marrow cells were incubated for 6 days in RPMI 1640 Glutamax I (Gibco), 10% fetal calf serum, 30% L929 supernatant [as macrophage colony-stimulating factor (M-CSF) source]. The bone marrow–derived macrophages (BMDMs) were seeded (16 hours) in six-well plates (3×10^5 cells per well) in RPMI, 3.3% FCS, and 5% L929 supernatant. BMDMs were incubated with live Gram-positive (*Enterococcus* subsp. isolated from mouse intestine) or Gram-negative (*E. coli* DH5α) bacteria (8 hours), after which cell culture supernatant was collected and centrifuged (5 min, 1200 rpm, 4°C) to remove cells and bacteria (5 min, 10,000 rpm, 4°C). Cell-free supernatants were stored at −80°C until used. Hepa1-6 cells (C57L mouse hepatoma; American Type Culture Collection) were seeded in DMEM (Invitrogen), 10% FCS, penicillin, and streptomycin (20 U/ml, Invitrogen). All cells were incubated at 37°C, 95% humidity, and 5% CO_2.

Protoporphyrins

Heme (iron protoporphyrin; FePPIX; Frontier Scientific) and protoporphyrin IX (protoporphyrin IX disodium salt; NaPPIX; Frontier Scientific) were dissolved in 0.2 M HCl, and pH was adjusted to 7.4 with sterile 0.2 M NaOH.

Primary hepatocytes

Primary mouse hepatocytes were isolated as described (*36*). Briefly, livers from naïve BALB/c mice were perfused through the portal vein (5 ml/min, 10 min, 37°C) with liver perfusion medium (Invitrogen), and the tissue was disrupted. Cells were filtered (100 μm), washed (William's E medium; 4% FCS) (Invitrogen), pelleted (100*g*, 30 s, 20°C), and resuspended (William's E medium, 4% FCS). Hepatocytes were isolated in a Percoll gradient (1.06/1.08/1.12 g/ml; 750*g*, 20 min, 20°C) (GE Healthcare), resuspended (William's E medium; 4% FCS), centrifuged (2 × 200*g*, 10 min, 4°C), resuspended (William's E medium; 4% FCS), and seeded onto gelatin (0.2%)–coated plates. The medium was replaced after 4 hours, and experiments were performed 24 to 48 hours thereafter. Primary human hepatocytes were cultured in hepatocyte culture medium as detailed by the supplier (Lonza).

Heme sensitization assays

Hepatocytes were seeded and exposed to heme (5 μM, 1 hour) in Hanks' Balanced Salt Solution (Invitrogen) without serum to avoid potential heme scavenging by serum proteins, as described (*8*). Subsequently, hepatocytes were washed (PBS) and challenged in Dulbecco's modified Eagle's medium, 10% FCS (Hepa1-6), or 4% FCS (primary hepatocytes), with human recombinant TNF (5 to 40 ng/ml, 3 to 16 hours; R&D Systems), Fas ligand (Jo2 antibody against CD 95, 0.5 μg/ml, 4 hours; BD Biosciences), H_2O_2 (125 μM, 8 hours; Sigma), or 3-morpholinosydnonimine (SIN-1; 100 μM, 24 hours; Sigma). Cell viability was assessed by crystal violet assay, as described (*37*). Heme (FePPIX; Frontier Scientific) was dissolved in sterile 0.2 M NaOH at alkaline pH and adjusted to pH 7.4 with sterile 0.2 M HCl. Iron-free protoporphyrin (NaPPIX, Frontier Scientific) was dissolved in sterile 0.2 M HCl at acidic pH, and pH was adjusted to 7.4 with sterile 0.2 M NaOH. Aliquots were stored at −80°C until use.

Cytokines and NO measurements

TNF, IL-6 and IL-10 were quantified by enzyme-linked immunosorbent assay (ELISA) according to the manufacturer's instructions (Becton Dickinson). NO was measured with a Griess colorimetric assay (*38*).

CLP

CLP was performed as described elsewhere (*39*, *40*). Briefly, mice were anesthetized [ketamine (120 mg/kg)/xylazine (16 mg/kg) intraperitoneally (ip)]. Under sterile conditions, a 1-cm incision was made parallel to the midline, and the cecum was exteriorized and ligated

(sterile 3-0 Mersilk sutures; Ethicon) immediately distal to the ileocecal valve (reducing the lumen by 50 to 60% for low-grade CLP and 80 to 90% for high-grade CLP). The cecum was punctured once with a 23-gauge needle (low-grade CLP) or twice with a 21-gauge needle (high-grade CLP) and its content was extruded by applying pressure and reinserted into the abdominal cavity. The peritoneal wall was sutured with sterile 3-0 Dafilon sutures (Braun) and the skin was closed with a surgical staple (Autoclip 9 mm; Becton Dickinson). A single dose of saline was injected subcutaneously (1 ml per animal) for fluid resuscitation. After the surgical procedure, animals were maintained at 37°C (30 min) and received antibiotics intraperitoneally (imipenem-cilastatin, Tienam, MSD; 0.5 mg per animal) 2 hours after the surgical procedure and every 12 hours during 72 hours.

Colony-forming units

Peritoneal fluid was obtained by peritoneal lavage with 5 ml of sterile PBS (Sigma). Organs were weighed and homogenized under sterile conditions in 0.5 ml of PBS with Dounce tissue grinders (Sigma). Serial dilutions of blood, peritoneal lavage, and homogenized organs were immediately plated on Trypticase Soy Agar II plates supplemented with 5% Sheep Blood (Becton Dickinson). CFUs were counted after 24 hours of incubation at 37°C.

cDNA synthesis and LightCycler analysis

Total RNA was extracted with RNeasy Protect Mini Kit (Qiagen) and reverse-transcribed (SuperScriptII RNase H^- reverse transcriptase; Invitrogen) with random hexamer primers (Invitrogen) as follows: 70°C for 10 min, 37°C for 50 min, and 95°C for 5 min (RoboCycler Stratagene). HO-1 primers are 5′-TCTCAGGGGGTCAGGTC-3′ (forward) and 5′-GGAGCGGTGTCTGGGATG-3′ (reverse). The reaction was carried out with 1 μl of cDNA and 3 pmol of each primer, 2 mM $MgCl_2$, and 1× FastStart DNA SYBR Green I mix (Roche). The thermal cycler program was composed of 1 cycle at 95°C for 10 min, 45 cycles at 95°C for 15 s, 58°C for 5 s, and 72°C for 16 s, with transition rates of 20°C/s. PCR products were quantified by LightCycler Real-Time quantitative PCR software (Roche). Cycle numbers in the log-linear phase were plotted against the logarithm of template DNA. External standardization was performed with full-length HO-1 cDNA. Hypoxanthine-guanine phosphoribosyltransferase (HPRT) was used to normalize cDNA levels (*41*).

Flow cytometry

Leukocytes were washed and blocked in calcium- and magnesium-free PBS containing 2% FCS (v/v). After incubation (30 min, 4°C) with fluorochrome-conjugated monoclonal antibodies directed against CD11b (clone M1/70), IAd (clone AMS-32.1), GR1 (clone 1A8), CD49b (clone DX5), α/βTCR (clone H57-597), or CD19 (clone 1D3) (BD Biosciences, Pharmingen), cells were washed twice with PBS and 2% FCS (v/v) and acquired in a FACScan or FACSCalibur with CellQuest software (BD Biosciences). Dead cells were excluded from the analysis with propidium iodide. Analysis was done with FlowJo software (Tree Star Inc.). Cellular free radical generation was determined by incubating cells (10 μM, 15 min, 37°C, 95% humidity, 5% CO_2) with the broad free radical probe 5-(and 6)-chloromethyl-2′7′-dichlorodihydrofluoscein diacetate acetyl ester (CM-H_2DCFDA; Molecular Probes).

Immunofluorescence

Hepa1-6 cells, seeded and treated (as described above) on glass cover slips (Paul Marienfeld GmbH & Co.), were fixed (4% paraformaldehyde, 30 min), permeabilized (0.1% Triton X-100, 20 min), blocked (PBS, 10% goat serum, 20 min), and incubated overnight at 4°C with rabbit antibody against human HMGB1 (Abcam, ab18256; 0.5 μg/ml) or control rabbit IgG (Sigma) in PBS and 10% goat serum. Alexa 568–conjugated goat antibody against rabbit IgG (5 μg/ml; Invitrogen) was used as secondary antibody. Nuclear DNA was stained with Hoechst 33342 (10 μg/ml, PBS, 20 min; Invitrogen), and cells were mounted in Vectashield (Vector Laboratories). Images were captured with a fluorescence microscope (Leica, DMRA2) equipped with UV light and Evolution MP 5.0 Color Camera (Media Cybernetics). Images were analyzed with ImageJ software (National Institutes of Health).

Histology and immunohistology

Tissue samples were processed and stained essentially as described (*42*). HMGB1 was detected in paraffin-embedded, formalin-fixed sections (5 μm) after microwave antigen retrieval [0.01 M citrate buffer (pH 6.0) 20 min] with rabbit antibody against human HMGB1 (Becton Dickinson, 556528) (0.5 μg/ml, 4°C, overnight). Rabbit IgG was detected with biotin-conjugated donkey antibody against rabbit secondary antiserum (1:1000; Jackson Immunoresearch) and streptavidin-conjugated horseradish peroxidase amplification kit (Vectastain Elite ABC Kit, Vector Labs). Signal was revealed with 3,3′-diaminobenzidine (DAB). Sections were counterstained with Harris hematoxylin. Negative controls were performed by omitting the primary antibody or with a nonspecific rabbit polyclonal antibody. Images were obtained and analyzed as described above.

Serum biochemistry

Blood was collected in tubes with heparin after cardiac puncture, centrifuged (2 × 5 min, 1600*g*). AST, BUN, and CPK were measured according to the protocols of the International Federation of Clinical Chemistry, as described (*43*–*45*), by spectrophotometric analysis (modular DP; Roche-Hitachi, Echevarne Laboratories). Plasma HPX and haptoglobin were determined by ELISA (Life Diagnostics). Plasma hemoglobin was determined by spectroscopy at a wavelength of 577 nm (λ_{577}). Total plasma heme was measured with the 3,3′,5,5′ tetramethylbenzidine (TMB) peroxidase assay (BD Biosciences) at λ_{655}. Purified hemoglobin was used as standard for plasma hemoglobin and heme measurements. Blood smears were fixed in methanol and stained with Giemsa stain, and images were obtained and analyzed as described above.

HPX

Intact apo-HPX was isolated from rabbit serum as described (*46*). Purified HPX binds heme as assessed by absorbance and circular dichroism spectroscopy of the apoprotein or the oxidized and reduced heme-HPX complexes; the concentration of the protein and equimolar heme binding were quantified with published procedures and extinction coefficients (*47*). Neither the apo-HPX nor the heme-HPX complex is toxic for cells in vitro even at high concentrations (*48*). Mice received purified HPX (50 mg/kg ip) at 2, 12, 24, and 36 hours after CLP.

Western blotting

Proteins were prepared and subjected to electrophoresis essentially as described before (*49*). For HMGB1 detection in peritoneal fluid and in serum, samples were ultrafiltered with Centricon 100 columns (Millipore) and precipitated with trichloroacetic acid (TCA), washed twice in acetone, dried, dissolved in urea (8 M), and added to SDS–

polyacrylamide gel electrophoresis (SDS-PAGE) loading buffer. Primary hepatocyte and Hepa1-6 culture supernatants were concentrated on Vivaspin 500 columns (10-kD molecular mass cutoff; Vivascience AG) resulting in up to ~10-fold concentration. HMGB1 was detected with polyclonal antibody (Abcam, ab18256; 0.1 μg/ml). HO-1 was detected with a rabbit polyclonal antibody against human HO-1 (1:2.500; SPA-895, StressGen). Monoclonal antibodies were used to detect α-tubulin (T9026, 1:5.000 dilution; Sigma) and inducible NO synthase (Becton Dickinson). Primary antibodies were detected with horseradish peroxidase–conjugated donkey antibody against rabbit, goat antibody against mouse, or rabbit antibody against mouse IgG secondary antibodies (Pierce, Rockford). Peroxidase activity was visualized with the SuperSignal chemiluminescent detection kit (Pierce) according to the manufacturer's instructions and stored in the form of photoradiographs (BiomaxTMMS, Eastman Kodak) or with the Image Station 440CF (Kodak). Digital images were obtained with an image scanner equipped with Adobe Photoshop software.

Septic shock patients

We analyzed the plasma concentration of HPX in 52 patients undergoing septic shock, as defined by the American College of Chest Physicians (ACCP)–Society of Critical Care Medicine (SCCM) consensus criteria (*22*). Patients were treated according to standard recommendations (*50*), including aggressive fluid resuscitation, broad-spectrum antibiotic therapy over the first 24 hours, vasoactive agents, and at least one intravenous dose of hydrocortisone. Blood samples were collected on the first, second, third, fifth, and seventh day after septic shock diagnosis. Blood was collected on ice between 1000 and 1200 hours with an arterial line or a peripheral vein, and plasma was collected by centrifugation (800*g*, 15 min, 4°C), aliquoted, and stored (−70°C) until analysis. Organ dysfunction was defined by the SOFA score on the basis of daily measurements (*23*). The outcome analyzed was 28th-day hospital mortality. The study protocol was approved by the institutional review board of each participating center (University Hospital of Federal University of Rio de Janeiro, Hospital Quinta D'Or, Casa de Saúde São José, Rio de Janeiro, Brazil). All patients, or their legal surrogates, gave written informed consent before any study-related procedures.

Statistical analysis

The comparison of two independent samples was assessed by the Student's *t* test and the Mann-Whitney test for Gaussian and non-Gaussian distributed samples, respectively. To compare more than two samples, we performed analysis of variance (ANOVA) or Kruskal-Wallis tests for Gaussian and non-Gaussian distributed samples, respectively. Comparison of different survival curves for the variously treated animals was done by the nonparametric log-rank test. For pairwise comparisons, the Bonferroni correction was used to ensure the overall significance level. Regression models were applied to describe genotype-based data, and statistical significance presented throughout the paper refers to additive effects. Kolmogorov-Smirnov and Shapiro-Wilk tests were performed to assess the normality of the samples under analysis. Regression models were applied to describe genotype-based data. In all data sets, the following model equation was applied: $Y = a + b \times \text{genotype} + c \times \text{heterozygote}$, where Y denotes the variable under analysis, with logarithmic transformation when appropriate; a is the baseline referring to the $Hmox1^{-/-}$ mean; b is the mean effect of adding an $Hmox1^{+/+}$ allele in the genotype (additive effect); c is the deviation of heterozygote mean from a single additive effect; genotype is an explanatory variable denoting the genotype coded as 0, 1, and 2 (0, 1, 2 $Hmox1^{+/+}$ alleles, respectively); and $Hmox1^{+/-}$ is the binary variable indicating the heterozygote genotype. Model validation was done by a thorough residual analysis, which included testing normality of the residuals and visual inspection of any trend in the residuals across genotypes. Statistical significance refers to additive effects in the regression analysis. Kolmogorov-Smirnov and Shapiro-Wilk tests were performed to infer whether data could come from normal distributions. All statistical tests were done at 5% significance level with InStat and R software (*51*).

For human data, a survival analysis was performed with the package available in the R software (*51*). For each patient, survival time was computed by the difference between the time of patient inclusion in the intensive care unit and the respective closing date of the hospital record. Patients that left hospital after treatment were considered as right-censored observations for the respective survival time. Because the survival time could be approximated by a lognormal distribution, several survival regression models based on such probability distributions were fitted to the data. HPX was included in the models as an explanatory variable with either the first or the last time point measure available for a patient. The statistical significance of this explanatory variable in the models was assessed by the traditional *z*-score tests. A correlation analysis between SOFA score and HPX at different time points was also performed with Spearman's coefficient.

SUPPLEMENTARY MATERIAL

www.sciencetranslationalmedicine.org/cgi/content/full/2/51/51ra71/DC1
Fig. S1. Effects of HO-1 on bacterial load.
Fig. S2. Modulation of cytokine production by HO-1.
Fig. S3. HO-1 regulates the production of NO in peritoneal macrophages.
Fig. S4. Red blood cell morphology in mice subjected to CLP.
Fig. S5. HO-1 modulates PMN cell activation in response to CLP.
Fig. S6. Infiltrating leukocytes after CLP.
Fig. S7. Adenoviral overexpression of HO-1 in hepatocytes.
Table S1. Characteristics of septic shock patients.
Table S2. Correlations between HPX serum concentration and SOFA.

REFERENCES AND NOTES

1. G. S. Martin, D. M. Mannino, S. Eaton, M. Moss, The epidemiology of sepsis in the United States from 1979 through 2000. *N. Engl. J. Med.* **348**, 1546–1554 (2003).
2. J. Cohen, The immunopathogenesis of sepsis. *Nature* **420**, 885–891 (2002).
3. R. Medzhitov, Origin and physiological roles of inflammation. *Nature* **454**, 428–435 (2008).
4. A. F. Read, A. L. Graham, L. Råberg, Animal defenses against infectious agents: Is damage control more important than pathogen control. *PLoS Biol.* **6**, e4 (2008).
5. J. Schafer, Tolerance to plant disease. *Annu. Rev. Phytopathol.* **9**, 235–252 (1971).
6. D. S. Schneider, J. S. Ayres, Two ways to survive infection: What resistance and tolerance can teach us about treating infectious diseases. *Nat. Rev. Immunol.* **8**, 889–895 (2008).
7. R. Medzhitov, Damage control in host–pathogen interactions. *Proc. Natl. Acad. Sci. U.S.A.* **106**, 15525–15526 (2009).
8. E. Seixas, R. Gozzelino, A. Chora, A. Ferreira, G. Silva, R. Larsen, S. Rebelo, C. Penido, N. R. Smith, A. Coutinho, M. P. Soares, Heme oxygenase-1 affords protection against noncerebral forms of severe malaria. *Proc. Natl. Acad. Sci. U.S.A.* **106**, 15837–15842 (2009).
9. R. Tenhunen, H. S. Marver, R. Schmid, The enzymatic conversion of heme to bilirubin by microsomal heme oxygenase. *Proc. Natl. Acad. Sci. U.S.A.* **61**, 748–755 (1968).
10. S. W. Chung, X. Liu, A. A. Macias, R. M. Baron, M. A. Perrella, Heme oxygenase-1–derived carbon monoxide enhances the host defense response to microbial sepsis in mice. *J. Clin. Invest.* **118**, 239–247 (2008).

11. R. Gozzelino, V. Jeney, M. P. Soares, Mechanisms of cell protection by heme oxygenase-1. *Annu. Rev. Pharmacol. Toxicol.* **50**, 323–354 (2010).
12. H. J. H. Fenton, Oxidation of tartaric acid in presence of iron. *J. Chem. Soc. Trans.* **65**, 899–910 (1894).
13. A. C. Chou, C. D. Fitch, Mechanism of hemolysis induced by ferriprotoporphyrin IX. *J. Clin. Invest.* **68**, 672–677 (1981).
14. A. Pamplona, A. Ferreira, J. Balla, V. Jeney, G. Balla, S. Epiphanio, A. Chora, C. D. Rodrigues, I. P. Gregoire, M. Cunha-Rodrigues, S. Portugal, M. P. Soares, M. M. Mota, Heme oxygenase-1 and carbon monoxide suppress the pathogenesis of experimental cerebral malaria. *Nat. Med.* **13**, 703–710 (2007).
15. M. J. Nielsen, S. K. Moestrup, Receptor targeting of hemoglobin mediated by the haptoglobins: Roles beyond heme scavenging. *Blood* **114**, 764–771 (2009).
16. E. Tolosano, S. Fagoonee, N. Morello, F. Vinchi, V. Fiorito, Heme scavenging and the other facets of hemopexin. *Antioxid. Redox Signal.* **12**, 305–320 (2010).
17. B. N. Porto, L. S. Alves, P. L. Fernández, T. P. Dutra, R. T. Figueiredo, A. V. Graça-Souza, M. T. Bozza, Heme induces neutrophil migration and reactive oxygen species generation through signaling pathways characteristic of chemotactic receptors. *J. Biol. Chem.* **282**, 24430–24436 (2007).
18. K. L. Rock, H. Kono, The inflammatory response to cell death. *Annu. Rev. Pathol.* **3**, 99–126 (2008).
19. H. Wang, O. Bloom, M. Zhang, J. M. Vishnubhakat, M. Ombrellino, J. Che, A. Frazier, H. Yang, S. Ivanova, L. Borovikova, K. R. Manogue, E. Faist, E. Abraham, J. Andersson, U. Andersson, P. E. Molina, N. N. Abumrad, A. Sama, K. J. Tracey, HMG-1 as a late mediator of endotoxin lethality in mice. *Science* **285**, 248–251 (1999).
20. R. Takamiya, C. C. Hung, S. R. Hall, K. Fukunaga, T. Nagaishi, T. Maeno, C. Owen, A. A. Macias, L. E. Fredenburgh, A. Ishizaka, R. S. Blumberg, R. M. Baron, M. A. Perrella, High-mobility group box 1 contributes to lethality of endotoxemia in heme oxygenase-1–deficient mice. *Am. J. Respir. Cell Mol. Biol.* **41**, 129–135 (2009).
21. J. M. Gutteridge, A. Smith, Antioxidant protection by haemopexin of haem-stimulated lipid peroxidation. *Biochem. J.* **256**, 861–865 (1988).
22. R. C. Bone, R. A. Balk, F. B. Cerra, R. P. Dellinger, A. M. Fein, W. A. Knaus, R. M. Schein, W. J. Sibbald, Definitions for sepsis and organ failure and guidelines for the use of innovative therapies in sepsis. The ACCP/SCCM Consensus Conference Committee. American College of Chest Physicians/Society of Critical Care Medicine. *Chest* **101**, 1644–1655 (1992).
23. R. Moreno, J. L. Vincent, R. Matos, A. Mendonca, F. Cantraine, L. Thijs, J. Takala, C. Sprung, M. Antonelli, H. Bruining, S. Willatts, The use of maximum SOFA score to quantify organ dysfunction/failure in intensive care. Results of a prospective, multicentre study. Working Group on Sepsis related Problems of the ESICM. *Intensive Care Med.* **25**, 686–696 (1999).
24. L. Råberg, D. Sim, A. F. Read, Disentangling genetic variation for resistance and tolerance to infectious diseases in animals. *Science* **318**, 812–814 (2007).
25. S. Bhakdi, H. Bayley, A. Valeva, I. Walev, B. Walker, M. Kehoe, M. Palmer, Staphylococcal alpha-toxin, streptolysin-O, and *Escherichia coli* hemolysin: Prototypes of pore-forming bacterial cytolysins. *Arch. Microbiol.* **165**, 73–79 (1996).
26. G. Silva, V. Jeney, A. Chora, R. Larsen, J. Balla, M. P. Soares, Oxidized hemoglobin is an endogenous proinflammatory agonist that targets vascular endothelial cells. *J. Biol. Chem.* **284**, 29582–29595 (2009).
27. J. Bullen, E. Griffiths, H. Rogers, G. Ward, Sepsis: The critical role of iron. *Microbes Infect.* **2**, 409–415 (2000).
28. A. Ferreira, J. Balla, V. Jeney, G. Balla, M. P. Soares, A central role for free heme in the pathogenesis of severe malaria: The missing link? *J. Mol. Med.* **86**, 1097–1111 (2008).
29. X. Liang, T. Lin, G. Sun, L. Beasley-Topliffe, J. M. Cavaillon, H. S. Warren, Hemopexin down-regulates LPS-induced proinflammatory cytokines from macrophages. *J. Leukoc. Biol.* **86**, 229–235 (2009).
30. M. P. Soares, F. H. Bach, Heme oxygenase-1: From biology to therapeutic potential. *Trends Mol. Med.* **15**, 50–58 (2009).
31. K. D. Poss, S. Tonegawa, Reduced stress defense in heme oxygenase 1-deficient cells. *Proc. Natl. Acad. Sci. U.S.A.* **94**, 10925–10930 (1997).
32. M. J. Tracz, J. P. Juncos, A. J. Croatt, A. W. Ackerman, J. P. Grande, K. L. Knutson, G. C. Kane, A. Terzic, M. D. Griffin, K. A. Nath, Deficiency of heme oxygenase-1 impairs renal hemodynamics and exaggerates systemic inflammatory responses to renal ischemia. *Kidney Int.* **72**, 1073–1080 (2007).
33. P. Wiesel, A. P. Patel, N. DiFonzo, P. B. Marria, C. U. Sim, A. Pellacani, K. Maemura, B. W. LeBlanc, K. Marino, C. M. Doerschuk, S. F. Yet, M. E. Lee, M. A. Perrella, Endotoxin-induced mortality is related to increased oxidative stress and end-organ dysfunction, not refractory hypotension, in heme oxygenase-1–deficient mice. *Circulation* **102**, 3015–3022 (2000).
34. S. Takaki, N. Takeyama, Y. Kajita, T. Yabuki, H. Noguchi, Y. Miki, Y. Inoue, T. Nakagawa, H. Noguchi, Beneficial effects of the heme oxygenase-1/carbon monoxide system in patients with severe sepsis/septic shock. *Intensive. Care. Med.* **36**, 42–48 (2010).
35. S. F. Yet, M. A. Perrella, M. D. Layne, C. M. Hsieh, K. Maemura, L. Kobzik, P. Wiesel, H. Christou, S. Kourembanas, M. E. Lee, Hypoxia induces severe right ventricular dilatation and infarction in heme oxygenase-1 null mice. *J. Clin. Invest.* **103**, R23–R29 (1999).
36. L. A. Gonçalves, A. M. Vigário, C. Penha-Gonçalves, Improved isolation of murine hepatocytes for in vitro malaria liver stage studies. *Malar. J.* **6**, 169 (2007).
37. M. P. Soares, M. P. Seldon, I. P. Gregoire, T. Vassilevskaia, P. O. Berberat, J. Yu, T. Y. Tsui, F. H. Bach, Heme oxygenase-1 modulates the expression of adhesion molecules associated with endothelial cell activation. *J. Immunol.* **172**, 3553–3563 (2004).
38. J. P. Griess, On a new series of bodies in which nitrogen is substituted for hydrogen. *Philos. Trans. R. Soc. Lond.* **154**, 667–731 (1864).
39. K. A. Wichterman, A. E. Baue, I. H. Chaudry, Sepsis and septic shock—A review of laboratory models and a proposal. *J. Surg. Res.* **29**, 189–201 (1980).
40. K. M. McMasters, W. G. Cheadle, Regulation of macrophage TNFα, IL-1β, and Ia (I-Aα) mRNA expression during peritonitis is site dependent. *J. Surg. Res.* **54**, 426–430 (1993).
41. J. McDaid, K. Yamashita, A. Chora, R. Ollinger, T. B. Strom, X. C. Li, F. H. Bach, M. P. Soares, Heme oxygenase-1 modulates the allo-immune response by promoting activation-induced cell death of T cells. *FASEB. J.* **19**, 458–460 (2005).
42. K. Sato, J. Balla, L. Otterbein, R. N. Smith, S. Brouard, Y. Lin, E. Czismadia, J. Sevigny, S. C. Robson, G. Vercellotti, A. M. K. Choi, F. H. Bach, M. P. Soares, Carbon monoxide generated by heme oxygenase-1 suppresses the rejection of mouse-to-rat cardiac transplants. *J. Immunol.* **166**, 4185–4194 (2001).
43. H. U. Bergmeyer, M. Horder, R. Rej, International Federation of Clinical Chemistry (IFCC) Scientific Committee, Analytical Section: Approved recommendation (1985) on IFCC methods for the measurement of catalytic concentration of enzymes. Part 2. IFCC method for aspartate aminotransferase (L-aspartate: 2-oxoglutarate aminotransferase, EC 2.6.1.1). *J. Clin. Chem. Clin. Biochem.* **24**, 497–510 (1986).
44. H. U. Bergmeyer, M. Horder, R. Rej, International Federation of Clinical Chemistry (IFCC) Scientific Committee, Analytical Section: Approved recommendation (1985) on IFCC methods for the measurement of catalytic concentration of enzymes. Part 3. IFCC method for alanine aminotransferase (L-alanine: 2-oxoglutarate aminotransferase, EC 2.6.1.2). *J. Clin. Chem. Clin. Biochem.* **24**, 481–495 (1986).
45. M. Hørder, R. C. Elser, W. Gerhardt, M. Mathieu, E. J. Sampson, International Federation of Clinical Chemistry, Scientific Division Committee on Enzymes: Approved recommendation on IFCC methods for the measurement of catalytic concentration of enzymes. Part 7. IFCC method for creatine kinase (ATP: creatine *N*-phosphotransferase, EC 2.7.3.2). *Eur. J. Clin. Chem. Clin. Biochem.* **29**, 435–456 (1991).
46. A. Smith, W. T. Morgan, Transport of heme by hemopexin to the liver: Evidence for receptor-mediated uptake. *Biochem. Biophys. Res. Commun.* **84**, 151–157 (1978).
47. J. D. Eskew, R. M. Vanacore, L. Sung, P. J. Morales, A. Smith, Cellular protection mechanisms against extracellular heme. Heme-hemopexin, but not free heme, activates the N-terminal c-Jun kinase. *J. Biol. Chem.* **274**, 638–648 (1999).
48. R. C. Li, S. Saleem, G. Zhen, W. Cao, H. Zhuang, J. Lee, A. Smith, F. Altruda, E. Tolosano, S. Dore, Heme–hemopexin complex attenuates neuronal cell death and stroke damage. *J. Cereb. Blood Flow Metab.* **29**, 953–964 (2009).
49. G. Silva, A. Cunha, I. P. Gregoire, M. P. Seldon, M. P. Soares, The antiapoptotic effect of heme oxygenase-1 in endothelial cells involves the degradation of p38α MAPK isoform. *J. Immunol.* **177**, 1894–1903 (2006).
50. R. P. Dellinger, J. M. Carlet, H. Masur, H. Gerlach, T. Calandra, J. Cohen, J. Gea-Banacloche, D. Keh, J. C. Marshall, M. M. Parker, G. Ramsay, J. L. Zimmerman, J. L. Vincent, M. M. Levy, Surviving Sepsis Campaign guidelines for management of severe sepsis and septic shock. *Crit. Care Med.* **32**, 858–873 (2004).
51. http://www.r-project.org.

52. **Acknowledgments:** We thank S. F. Yet (Pulmonary and Critical Care Division, Brigham and Women's Hospital) for providing Hmox1 breeding pairs from which *Hmox1*$^{-/-}$ mice were derived; E. Tolosano (University of Torino, Torino, Italy) for critical review of the manuscript; S. Rebelo (Instituto Gulbenkian de Ciência) for invaluable help in breeding the *Hmox1*$^{-/-}$ mice; K. Rish, R. Lovelace, and R. Helston (University of Missouri) for technical expertise in the HPX isolation and characterization; and T. Davis (University of Missouri) for heme-HPX preparation. **Funding:** This work was supported by Fundação para a Ciência e Tecnologia (Portugal) grants SFRH/BPD/25436/2005 and PTDC/BIO/70815/2006 (to R.L.); SFRH/BPD/44256/2008 (to R.G.); SFRH/BD/11816/2003 (to L.T.); SFRH/BD/3106/2000 (to A.C.); SFRH/BPD/21707/2005 and PTDC/SAU MII/71140/ 2006 (to A.F.); SFHR/BD/33218/2007 (to I.M.); POCTI/SAU-MNO/56066/2004, POCTI/BIA-BCM/56829/2004, PTDC/BIA-BCM/101311/2008, and PTDC/SAU-FCF/100762/2008 (to M.P.S.); as well as GEMI Fund Linde Healthcare (to M.P.S.), the European Community, Sixth Framework grant LSH-2005-1.2.5-1 (to M.P.S.), and Marie Curie FP7-PEOPLE-2007-2-1-IEF, GASMALARIA (to V.J.). A.S. is supported by research incentive funds from the University of Missouri at Kansas City, MO, USA. F.A.B. is a research scholar supported by Conselho Nacional de Desenvolvimento Científico e Tecnológico and FAPERJ, Brazil. **Author contributions:** R.L. performed most of the experimental work with help from A.F. and S.C. R.G. performed the

experiments defining the cytotoxic effect of free heme. V.J. performed the experiments establishing heme and hemoglobin concentrations in plasma. A.C. and I.M. performed flow cytometry analysis. F.A.B. and A.M.J. conduced the clinical study with septic shock patients. M.M.C. and D.B. set up the CLP model in the laboratory. A.S. supplied the purified HPX and heme-HPX, gave critical advise on its use, and contributed to writing of the manuscript. M.P.S. formulated the hypothesis that free heme might play pivotal roles in the pathogenesis of severe sepsis, designed the experimental approach, and wrote the manuscript with help from R.L. R.L. and R. G. contributed to the study design. All authors read and approved the manuscript. **Competing interests:** The authors declare that they have no competing interests.

Submitted 29 March 2010
Accepted 3 September 2010
Published 29 September 2010
10.1126/scitranslmed.3001118

Citation: R. Larsen, R. Gozzelino, V. Jeney, L. Tokaji, F. A. Bozza, A. M. Japiassú, D. Bonaparte, M. M. Cavalcante, Â. Chora, A. Ferreira, I. Marguti, S. Cardoso, N. Sepúlveda, A. Smith, M. P. Soares, A central role for free heme in the pathogenesis of severe sepsis. *Sci. Transl. Med.* **2**, 51ra71 (2010).